Solution Combustion Synthesis

Impregnated Layer Combustion Synthesis is a Novel Methodology to Prepare Multi-Component Catalysts, Fundamentals and Experiments

University of Notre Dame

Department of Chemical and Biomolecular Engineering
University of Notre Dame

Outline:

- Overview of combustion synthesis
- Reaction system
- Combustion front analaysis
- Theoretical model results
- Conclusions
- Acknowledgements

Conventional Combustion System:

Characteristics:

- Exothermic nature of reaction
- High temperature (2000 ˚C)
- Short reaction time (~ sec)
- High temperature gradient (up to 10^6 K/s)

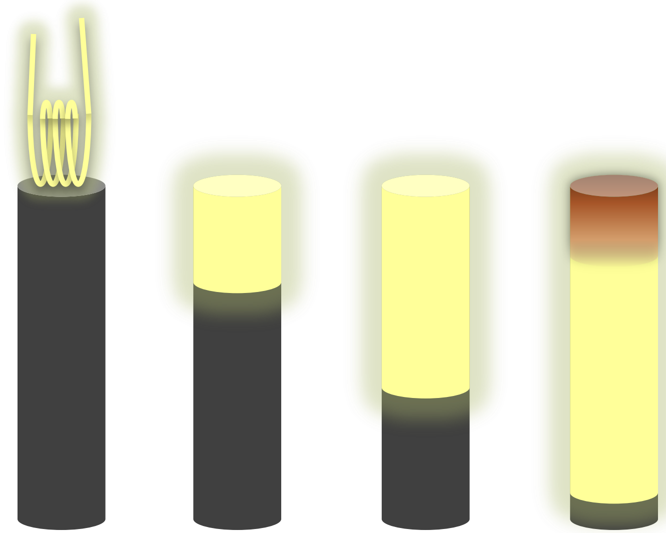

Self-Propagating High-Temperature Synthesis (SHS)

Example: TiC

Volume Combustion Synthesis (VCS)

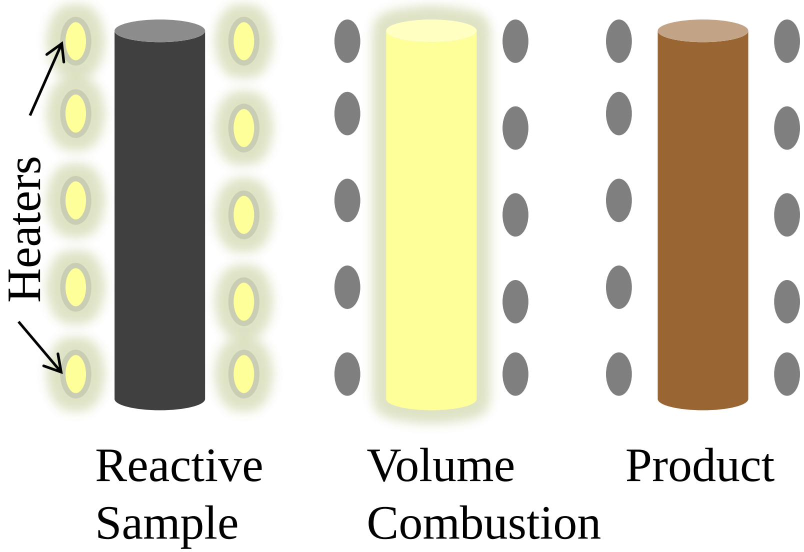

- Heterogeneous Systems
- Not suitable for nano-material synthesis

Solution Combustion Synthesis: nano-powders

- Molecular level homogenization
- High temperature (~1000 ˚C)
- Short process time
- Evolution of gases

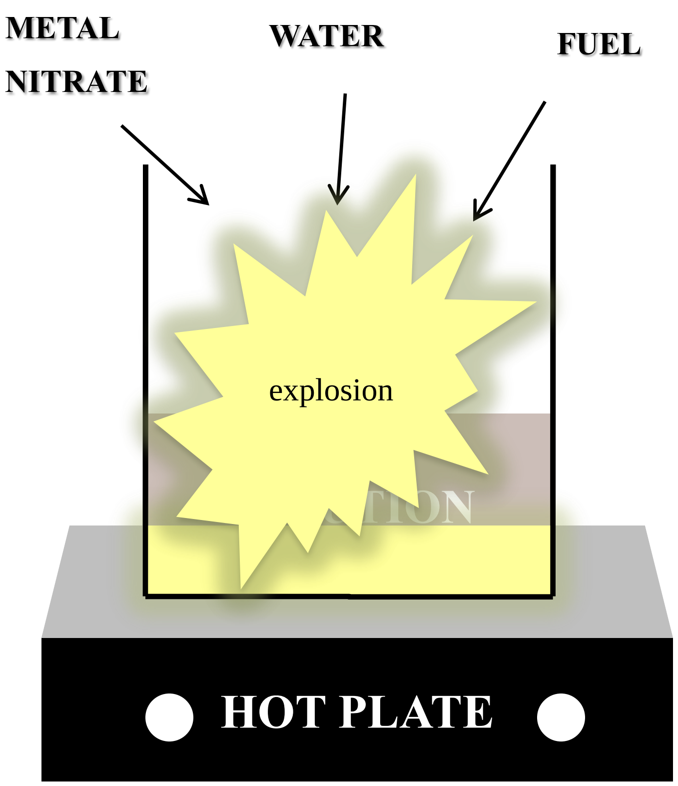

Porous, high surface area

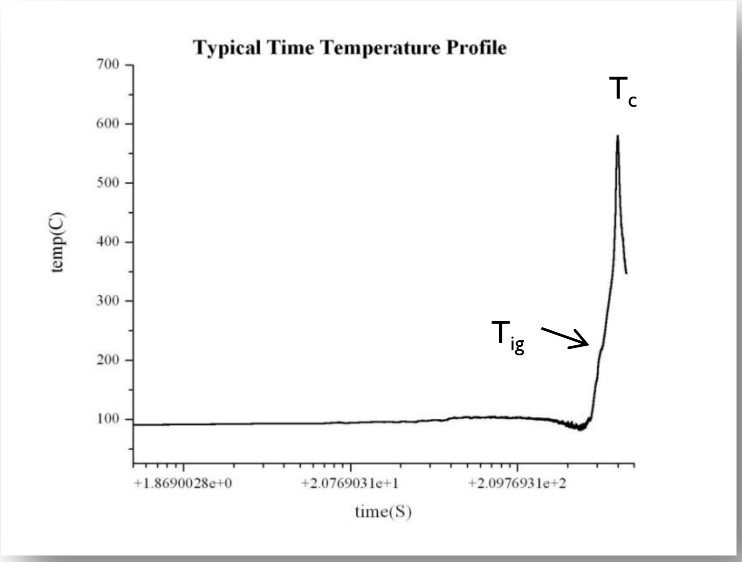

Explosive nature: less controllable

Impregnated Support Combustion Synthesis:

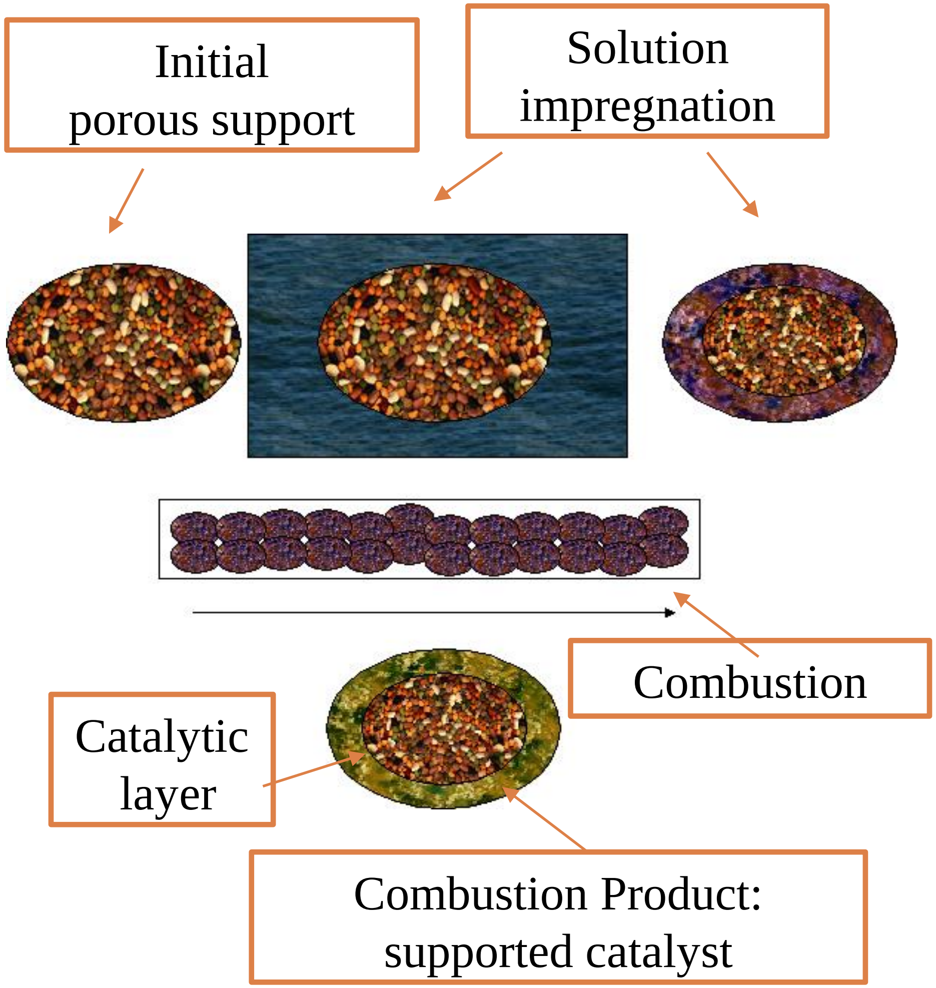

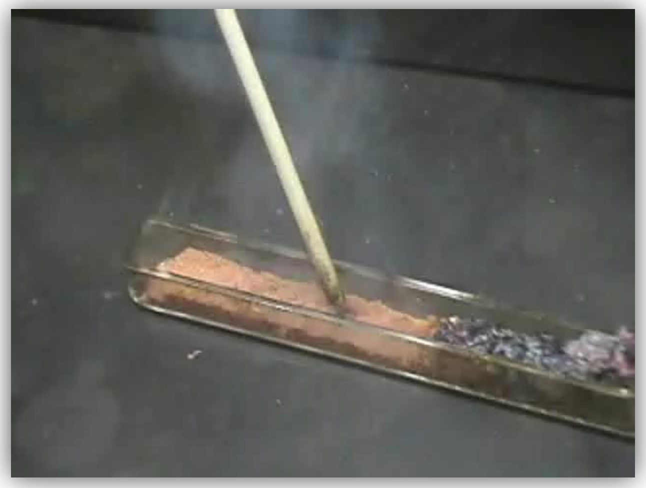

High specific surface
area of active sites

Impregnated Paper Combustion Synthesis:

- Reaction media is impregnated in a thin cellulose paper
- Eliminates the preheating stage
- Relatively low combustion temperature (~600 ˚C)
- Fast Cooling rate due to thin layer
- High product yield

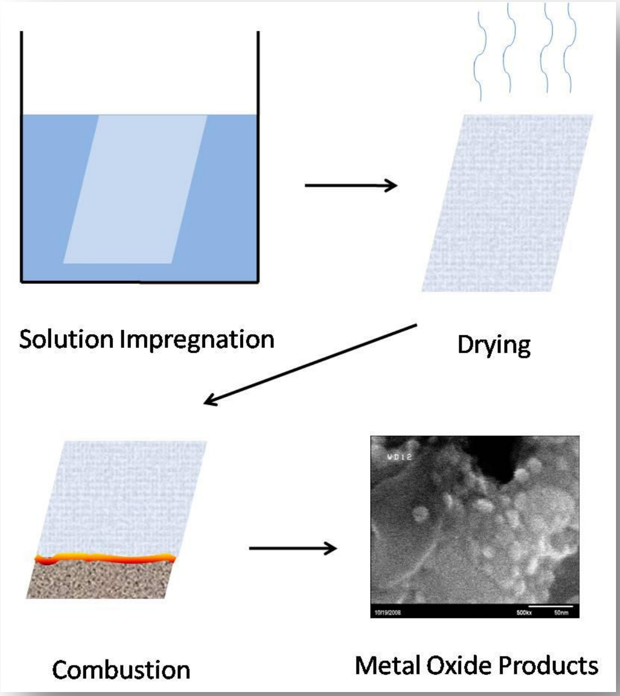

- Helps in achieving steady state propagation in weakly exothermic system.
- Continuous catalysts synthesis in stable conditions.

Ref: A. Kumar, A. S. Mukasyan, E. E. Wolf, *Appl. Catal. A: Gen.* **372** (2010), pp. 175-183

Catalyst Synthesis: reaction mixture

Metal Nitrate | Fuel: Glycine, Urea, Hydrazine… | Oxygen

$$Me^{v}(NO_3)_v + \tfrac{5}{9}\, v\, \varphi\, NH_2CH_2COOH + \tfrac{5}{4}\, v(\varphi-1)O_2$$

$$\downarrow$$

$$MeO_{v/2} + \tfrac{10}{9}\, v\, \varphi\, CO_2 + \tfrac{25}{18}\, v\, \varphi\, H_2O + \left\{\tfrac{(5\varphi-9)}{18}\right\} vN_2$$

Metal Oxide | Gas Phase products

$\varphi = 1$: stoichiometric

$\varphi > 1$: fuel rich

$\varphi < 1$: fuel lean

Catalyst Synthesis: combustion regimes

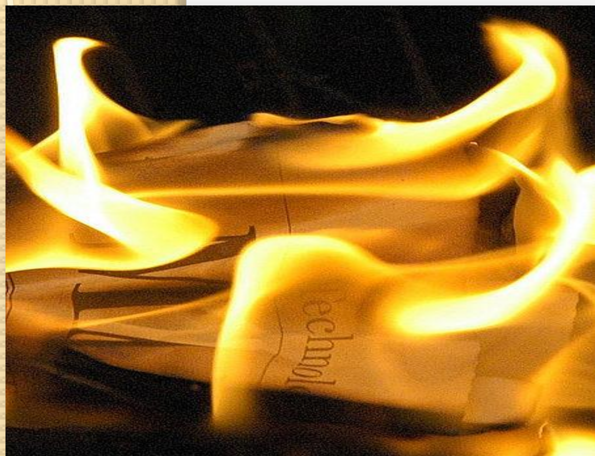

Flame mode

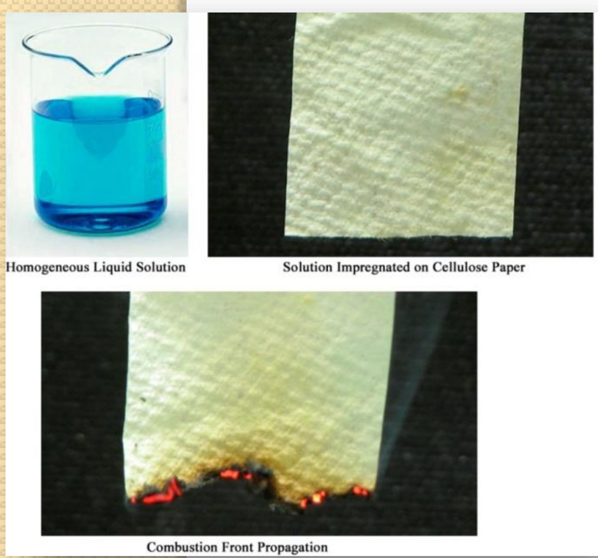

Smoldering mode

Cellulose Combustion Regimes:

- Flame : Uncontrolled, high temperature
- Smoldering : Controlled, low temperature

Decisive factors:

- Fuel layer thickness
- Oxygen concentration
- Heat transfer effects

Combustion Mode	Pure Cellulose	Impregnated Cellulose
Smoldering	No	Yes
Flame	Yes	Yes

Critical:
Temperature measurement

Catalyst Synthesis: thermal mapping

Temperature Measurement:

FLIR SC6000 HS

Time Resolution: up to 10 μ-sec

Spatial Resolution: 1.5 μm - 5 μm

Features:

Temperature Range: -10 °C to 1500 °C

Accuracy: ±2%

Repeatability: ±1%

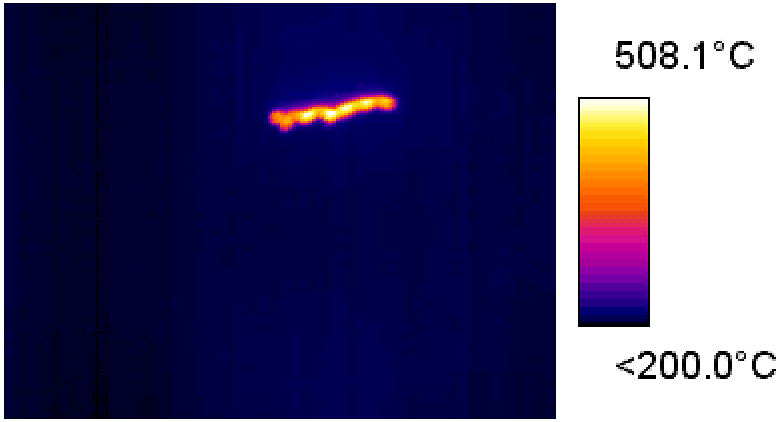

Combustion Front:

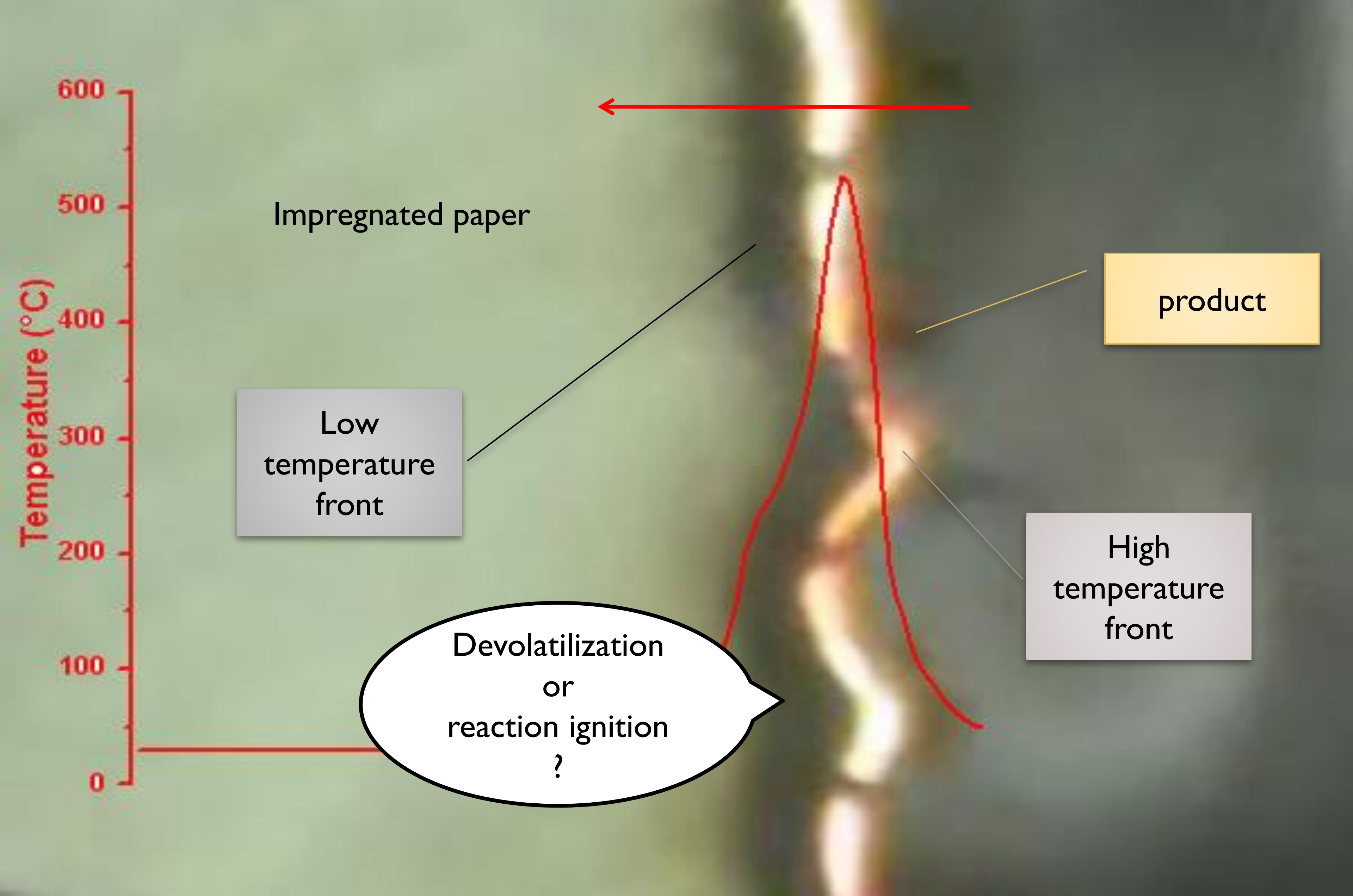

Combustion Front:

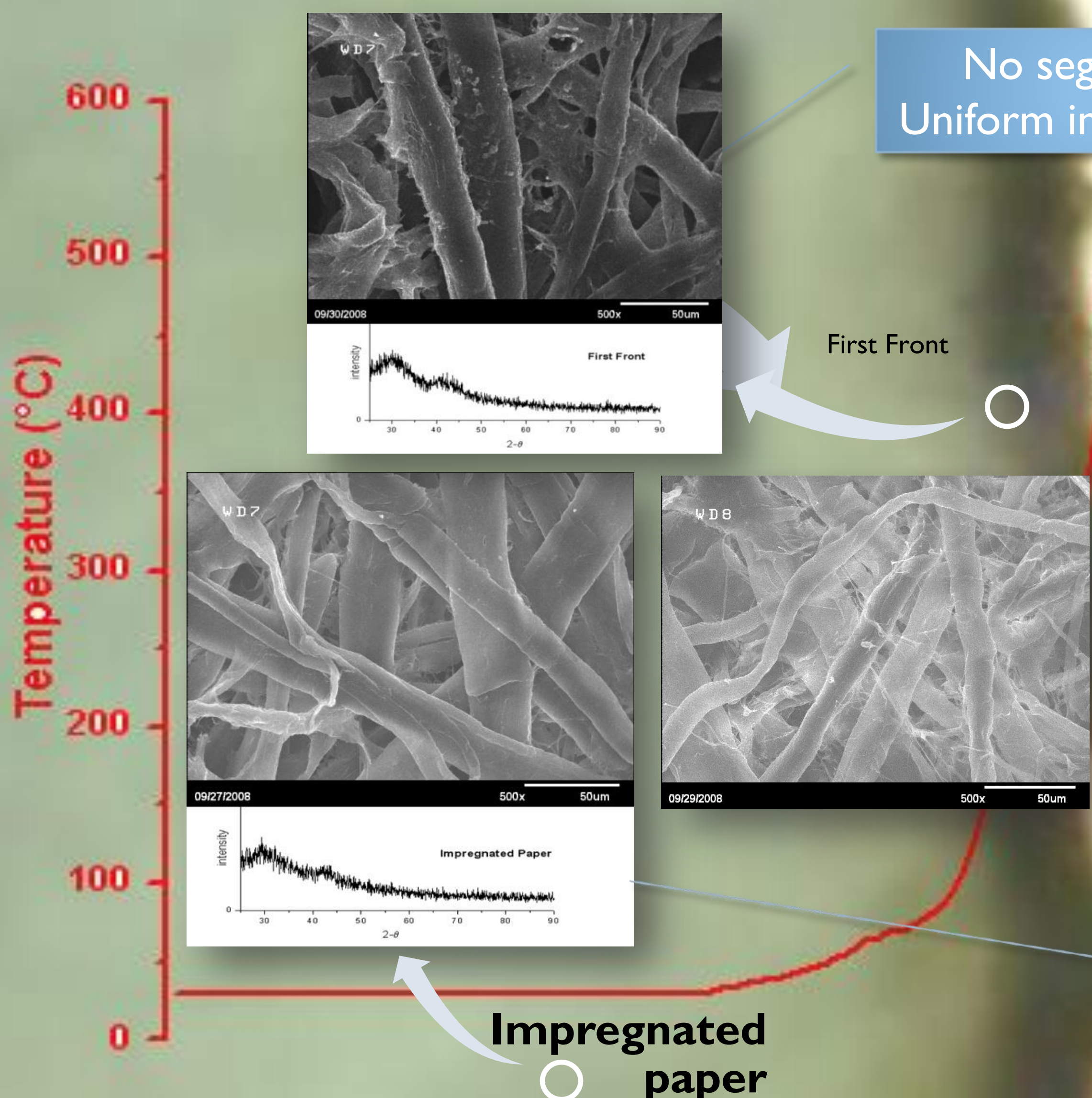

No segre
Uniform im

- No changes in cellulose structure
- No crystalline product

First Front: reactive mixture ignition

XRD
No crystalline form

Thermo Gravimetric Analysis:

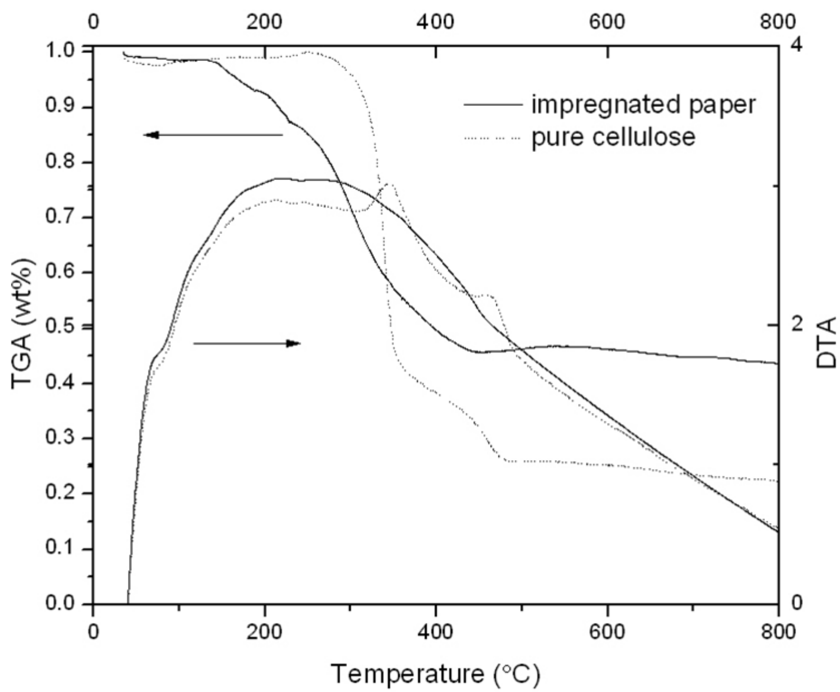

TGA RESULTS

Pure cellulose devolatilization starts at ~ 320 °C

Impregnated cellulose ignition ~ 140 °C

First Front: reactive mixture ignition

Combustion Front:

- **Change in cellulose structure**
- **Final product is crystalline**
- **Fine particles (~10 nm)**

Cellulose combustion

Smaller particle size (~10 nm)

Hollow tubes

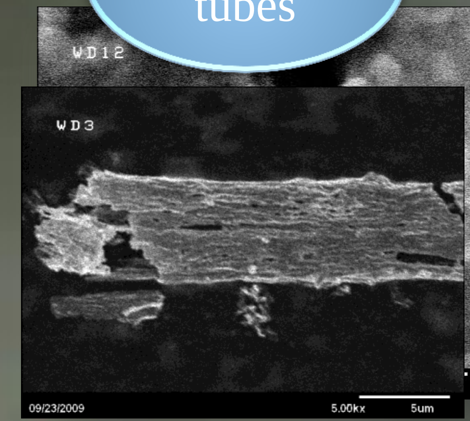

Product

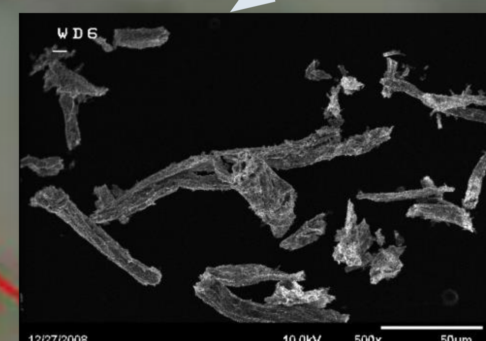

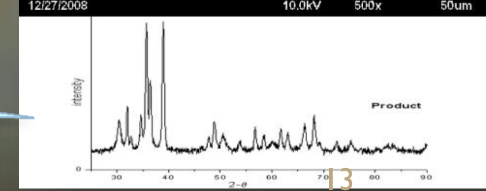

- **(1st + 2nd) wave in combination produce self propagation regimes**
- **2nd Wave provides the energy for calcination**

Crystalline product

Model Description

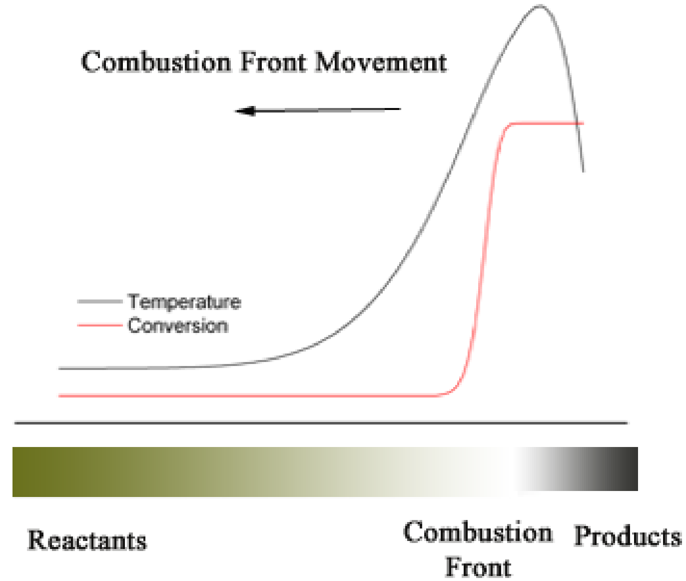

A(s) + B(s) ⟶ C(s) + $n_g \cdot D(g)$

Reactants:

$$\rho_1 c_{p1}\frac{\partial T}{\partial t} = \frac{\partial}{\partial x}\left(\lambda_1 \frac{\partial T}{\partial x}\right) + (-\Delta H_r) r(C_A, T) - \left(\frac{4U}{d}\right)_1 (T - T_0) - n_g r(C_A, T) c_p^g (T - T_0)$$

Products:

$$\rho_2 c_{p2}\frac{\partial T}{\partial t} = \frac{\partial}{\partial x}\left(\lambda_{p2} \frac{\partial T}{\partial x}\right) - \left(\frac{4U}{d}\right)_2 (T - T_0)$$

Where $\frac{\partial C_A}{\partial t} = -r(C_A, T)$ and $r(C_A, T) = k_0 C_A \exp\left(-\frac{E}{RT}\right)$

ICs: For $t \le 0, T = T_0, C_A = C_{A0};\ 0 < x < l$

BCs:

$-\lambda_2 \frac{\partial T}{\partial x} = q; 0 < t < t_q,\ x = 0$ and $\lambda_2 \frac{\partial T}{\partial x} = U(T - T_0);\ t > t_q, x = 0$

$-\lambda_1 \frac{\partial T}{\partial x} = U(T - T_0); t > 0, x = l$

Non-dimensional form of the equations: Dimensionless parameters

$$\theta = \frac{T}{T^*}, \quad \eta = 1 - \frac{C_A}{C_{A0}}, \quad \tau = \frac{t}{t^*}, \quad \xi = \frac{x}{x^*}, \quad t^* = \frac{\exp(\gamma)}{k_0}, \quad x^* = \left(\frac{\lambda_1 t^*}{\rho_1 c_{p1}}\right)^{\frac{1}{2}},$$

$$L = \frac{l}{x^*}, \quad \beta = \frac{(-\Delta H)C_{A0}}{c_{p1}\rho_1 T^*}, \quad \gamma = \frac{E}{RT^*},$$

$$\psi = \frac{qx^*}{\lambda_1 T^*}, \quad \alpha = \frac{\left(\frac{4U}{d}\right)_1 t^*}{c_{p1}\rho_1}, \quad Bi = \frac{Ux^*}{\lambda_1},$$

$$a_p = \begin{cases} 1 & \text{for reactants} \\ \dfrac{\left(\frac{\lambda_2}{\rho_2 c_{p2}}\right)}{\left(\frac{\lambda_1}{\rho_1 c_{p1}}\right)} & \text{for products} \end{cases}, \qquad \delta = \begin{cases} 1 & \text{for reactants} \\ \dfrac{\left(\frac{\left(\frac{U}{d}\right)_2}{\rho_2 c_{p2}}\right)}{\left(\frac{\left(\frac{U}{d}\right)_1}{\rho_1 c_{p1}}\right)} & \text{for products} \end{cases},$$

$$N_f = \frac{n_g c_p^g}{-\Delta H}, \quad \mu = \frac{\left(\frac{\left(\frac{U}{d}\right)_2 dx^*}{\lambda_2}\right)}{\left(\frac{\left(\frac{U}{d}\right)_1 dx^*}{\lambda_1}\right)}$$

where the subscripts 1 and 2 represent the reactants and the products respectively.

Final form of the equations:

Reactants:

$$\frac{\partial\theta}{\partial\tau} = \frac{\partial^2\theta}{\partial\xi^2} + \beta(1-\eta)\exp\left(\gamma\left(1-\frac{1}{\theta}\right)\right) - \alpha(T-T_0) - N_f\beta(1-\eta)\exp\left(\gamma\left(1-\frac{1}{\theta}\right)\right)$$

Products:

$$\frac{\partial\theta}{\partial\tau} = a_p\frac{\partial^2\theta}{\partial x^2} - \alpha\delta(T-T_0)$$

Where:

$$\frac{\partial\eta}{\partial\tau} = (1-\eta)\exp\left(\gamma\left(1-\frac{1}{\theta}\right)\right)$$

IC[s]:

$$\theta = \theta_0, \eta = 0;\ \tau \le 0,\ 0 < \xi < L$$

BC[s]:

$$-\frac{\partial\theta}{\partial\xi} = \psi; 0 < \tau < \tau_\psi,\ \xi = 0$$

$$\frac{\partial\theta}{\partial\xi} = \mu\cdot Bi(\theta-\theta_0);\ \tau > \tau_\psi,\ \xi = 0$$

$$-\frac{\partial\theta}{\partial\xi} = Bi(\theta-\theta_0);\ \tau > \tau_\psi,\ \xi = L$$

Model Results:

Temperature profile and combustion front with time

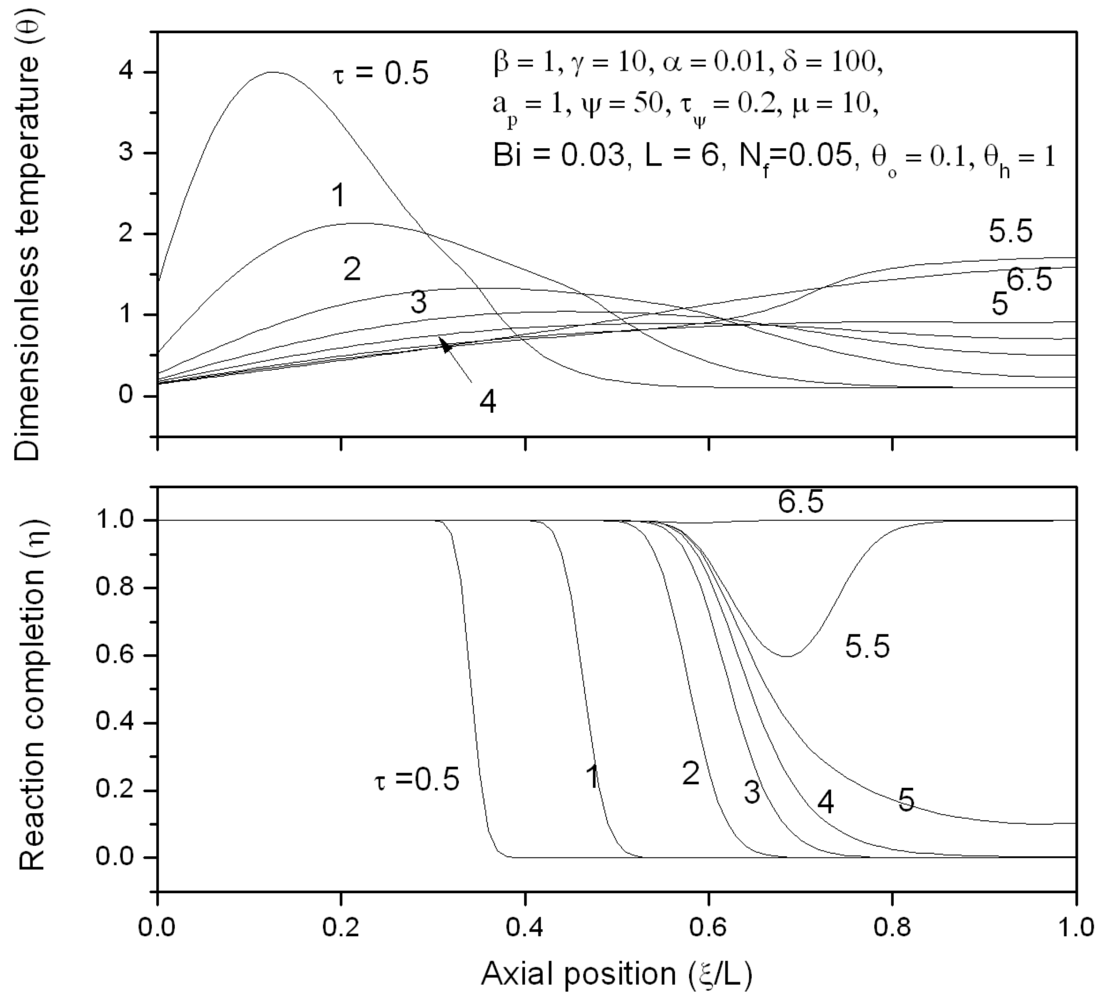

Effect of gas phase products:

Effect of gas phase products on combustion temperature profile

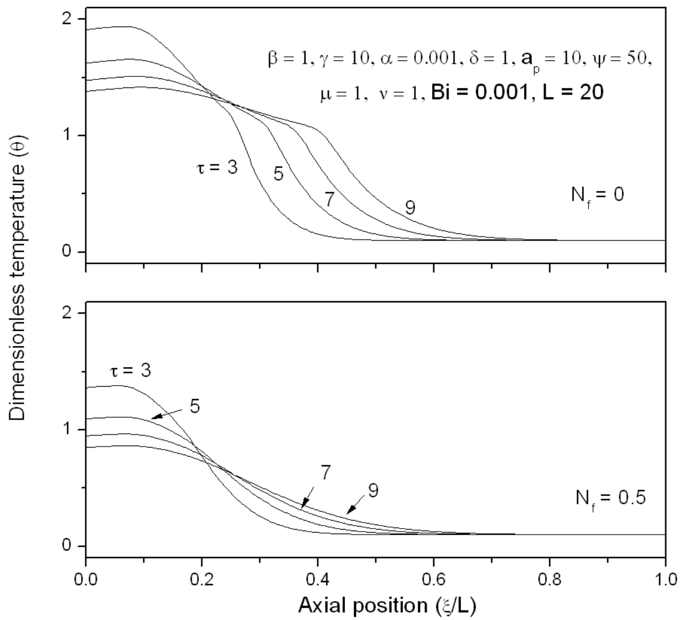

Location of combustion front with gas phase products

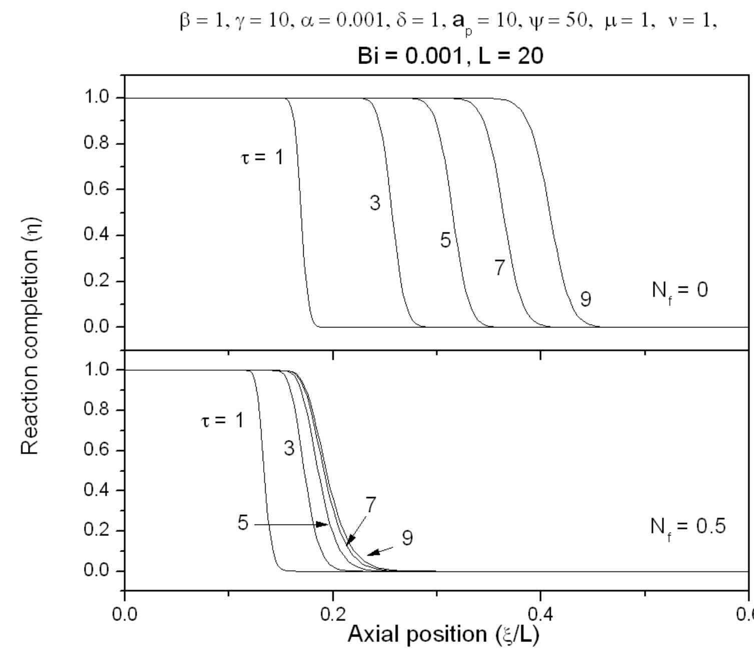

Gas phase products lower the combustion temperature as well as combustion front velocity

Effect of convective heat transfer: Due to change is surface area

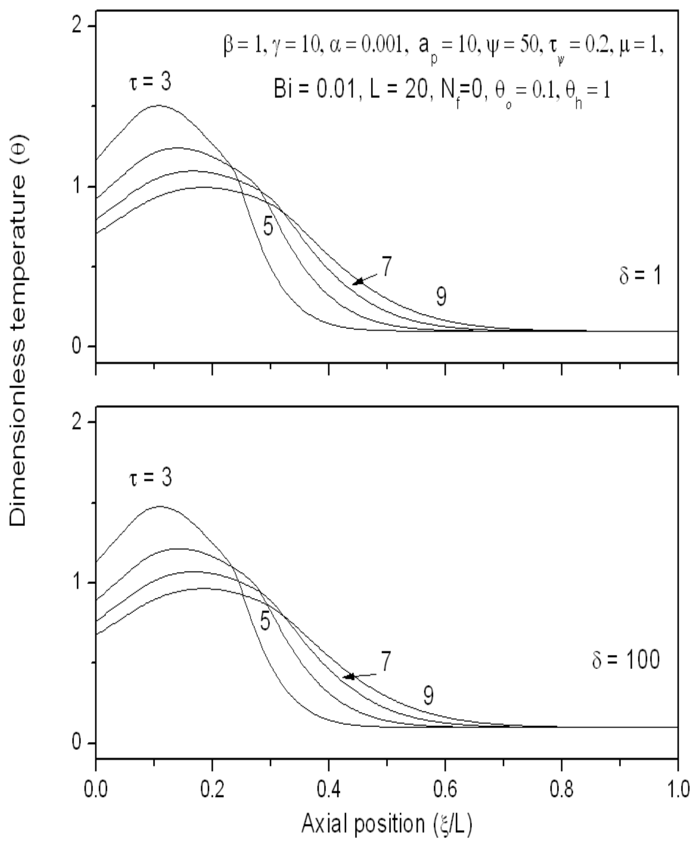

Effect of convective heat transfer on temperature profile

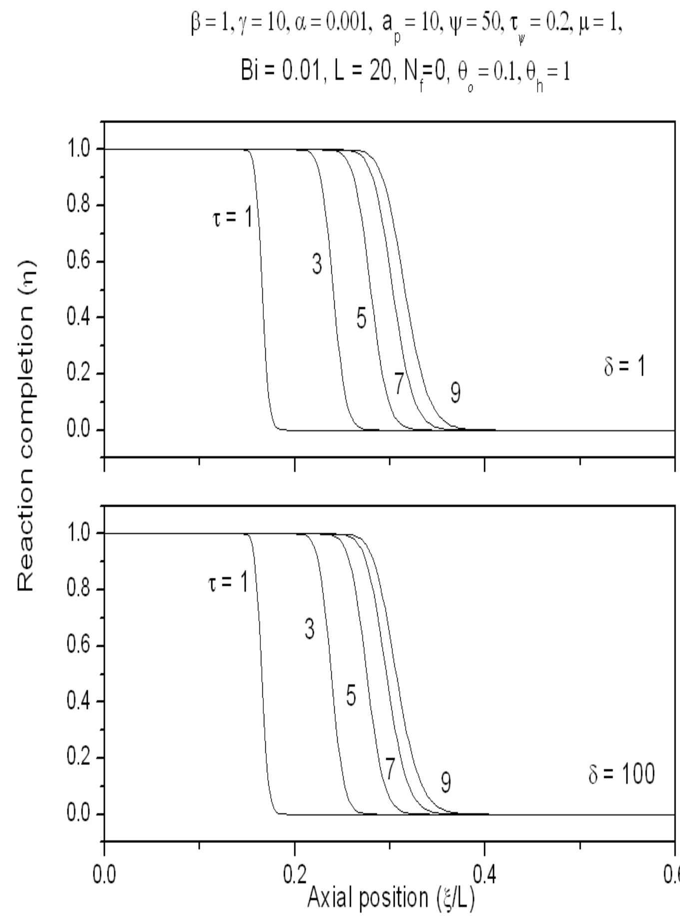

Effect of convective heat transfer on the location of combustion front

Combustion front temperature and velocity are not strongly dependent on surface area

Effect of change in Biot number:

Effect of heat loss on temperature profile due to change in Biot number

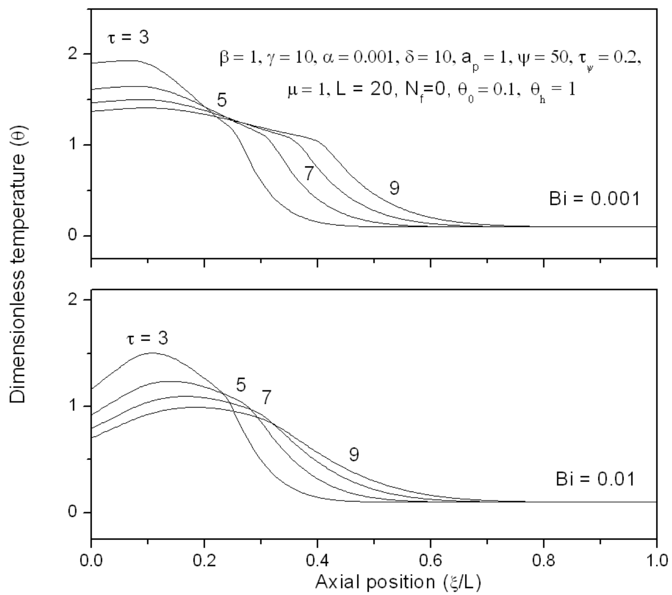

Effect on combustion front location due to change in Biot number

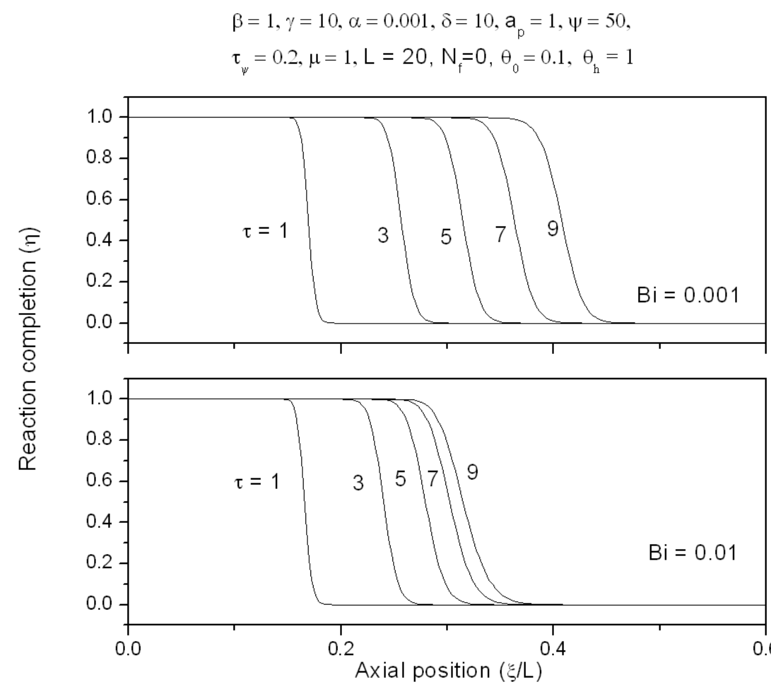

Increasing Bi# lowers the combustion temperature and combustion front velocity

Effect of change in thermal diffusivity:

Effect of thermal diffusivity on combustion temperature profile

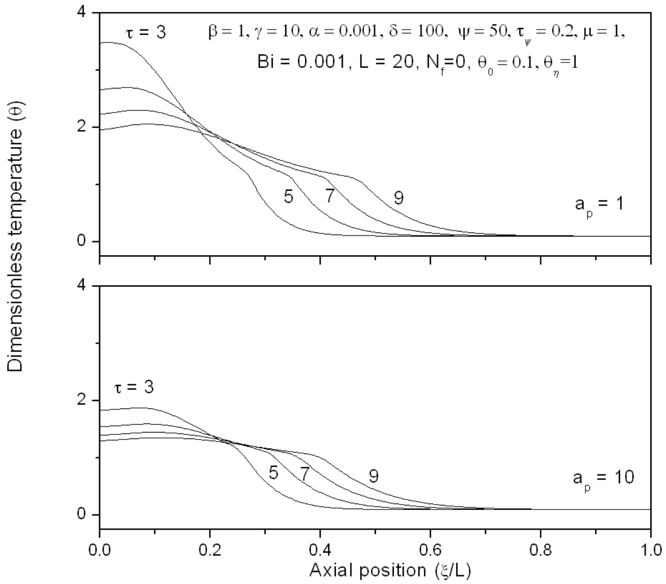

Effect of thermal diffusivity on the location of combustion front

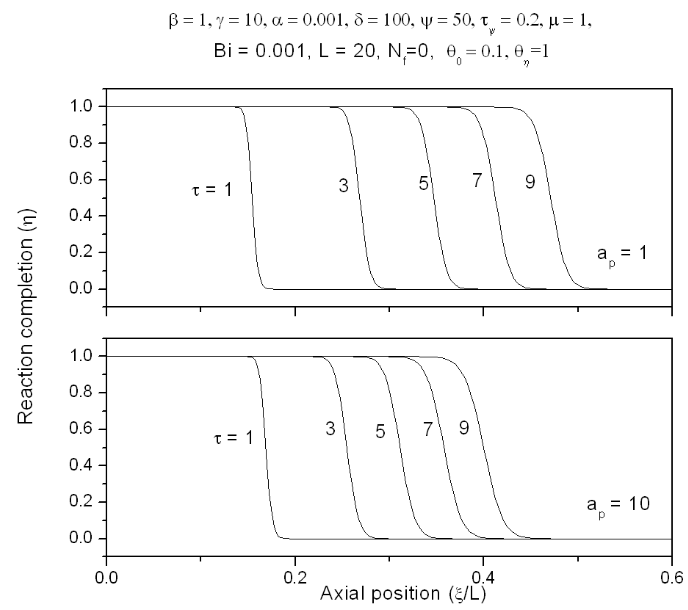

Increasing product thermal diffusivity lowers the combustion temperature and velocity

Summary: Model Results

- In a typical self propagating process, the product gases evolved reduce the combustion temperature and slow down the front velocity.
- The pores generated by these gases increase the total surface area and in turn further increases heat loss to the environment.
- High thermal diffusivity of the product decreases the combustion front velocity and increases the width of combustion peak.
- Heat loss from the product boundary increase the sharpness of the combustion peak.